

High-temperature kinetic magnetism in triangular lattices

Ivan Morera ^{1,2} Márton Kanász-Nagy,^{3,4} Tomasz Smolenski,⁵ Livio Ciorciaro ⁵ Ataç Imamoğlu ⁵ and Eugene Demler⁶

¹*Departament de Física Quàntica i Astrofísica, Facultat de Física, Universitat de Barcelona, E-08028 Barcelona, Spain*

²*Institut de Ciències del Cosmos, Universitat de Barcelona, ICCUB, Martí i Franquès 1, E-08028 Barcelona, Spain*

³*Max-Planck-Institut für Quantenoptik, Hans-Kopfermann-Strasse 1, 85748 Garching, Germany*

⁴*Munich Center for Quantum Science and Technology (MCQST), Schellingstrasse 4, D-80799 München, Germany*

⁵*Institute for Quantum Electronics, ETH Zürich, CH-8093 Zürich, Switzerland*

⁶*Institute for Theoretical Physics, ETH Zurich, Wolfgang-Pauli-Strasse 27, 8093 Zurich, Switzerland*



(Received 30 September 2022; revised 12 January 2023; accepted 6 May 2023; published 5 June 2023)

We study kinetic magnetism for the Fermi-Hubbard model in triangular lattices. We focus on the regime of strong interactions, $U \gg t$, and filling factors around one electron per site. For temperatures well above the hopping strength t , the Curie-Weiss form of the magnetic susceptibility suggests two complementary forms of kinetic magnetism. In the case of hole doping, antiferromagnetic polarons originate from kinetic frustration of individual holes, whereas for electron doping, Nagaoka-type ferromagnetic correlations are induced by propagating doublons. These results provide a possible theoretical explanation of recent experimental results in moiré transition metal dichalcogenide materials and cold atom systems. To understand many-body states arising from antiferromagnetic polarons at low temperatures, we study hole-doped systems in finite magnetic fields. At low dopings and intermediate magnetic fields, we find a magnetic polaron phase, separated from the fully polarized state by a metamagnetic transition. With decreasing magnetic field, the system shows a tendency to phase separate with hole-rich regions forming antiferromagnetic spin bags. We demonstrate that direct observations of magnetic polarons in triangular lattices can be achieved in experiments with ultracold atoms, which allow measurements of three point hole-spin-spin correlations.

DOI: [10.1103/PhysRevResearch.5.L022048](https://doi.org/10.1103/PhysRevResearch.5.L022048)

Introduction. Achieving electric control of magnetism is a long-standing goal in condensed-matter physics. Such systems will not only provide new insights into magnetism of itinerant electron systems, but also hold the promise of realizing new types of devices that combine long-term robustness of magnetic memory with the fast electric control [1,2]. One of the most studied examples of electrically controlled magnetism comes from magnetic semiconductors [3–13]. In this class of materials, conduction-band electrons control interaction between the localized spins and makes it possible to modify the ferromagnetic Curie transition temperature by applying a gate voltage [13,14]. Interplay of charge-carrier dynamics and magnetism is also crucial for understanding the rich phase diagram of colossal magnetoresistance manganite materials [15–18]. In this Letter, we discuss a different mechanism for electrical control of magnetism in which by changing charge-carrier concentration, one can tune between the antiferromagnetic and ferromagnetic interactions.

Our Letter builds upon earlier studies by Nagaoka [19] and Thouless [20], and Haerter and Shastry [21] of magnetism in Fermi-Hubbard-type models in the limit of large interaction strength U . Nagaoka's theorem states that on a square lattice the ground state of an almost half-filled Fermi-Hubbard

model with a single hole is a ferromagnetic state. Haerter and Shastry extended these arguments to triangular lattices and demonstrated that, for the same conditions, the ground state exhibits antiferromagnetic correlations. The key argument of our Letter is based on considering a Fermi-Hubbard model on triangular lattices in the regime when single-particle tunneling t is much smaller than the local interaction U , the band is close to half-filling, i.e., one electron per site ($\nu = 1$), and temperature is much higher than the superexchange energy $J = 4t^2/U$ but comparable to the single-particle tunneling t . Although naively, one expects to find no magnetic interactions in this regime at $\nu = 1$, we demonstrate that doping the system away from $\nu = 1$ introduces antiferro- and ferromagnetic interactions for hole and electron dopings, respectively. Our results are in good agreement with the observed magnetism in fermionic cold atom systems with a triangular optical lattice [22] and are consistent with the reported spin susceptibility measurements in transition-metal dichalcogenide (TMDC) moiré materials for $T \geq 4$ K [23]. In both cases, a transition between ferro- and antiferromagnetic interactions has been observed close to the filling factor $\nu = 1$ [22,23]. Moreover, a recent experiment with a TMDC moiré material has also observed the emergence of ferromagnetic correlations when the system is doped above half-filling [24]. Additionally, recent experiments and theoretical calculations have reported large values of on-site interaction $U/t \sim 20$ [23,25] which motivates us to focus on the $U/t \gg 1$ regime. Our work is also related to the recent observation of ferromagnetism in the Wigner crystal states of electrons at temperatures exceeding the expected superexchange interactions [26,27].

Published by the American Physical Society under the terms of the Creative Commons Attribution 4.0 International license. Further distribution of this work must maintain attribution to the author(s) and the published article's title, journal citation, and DOI.

Previous works have extensively studied the magnetic properties of the Fermi-Hubbard model in the triangular lattice at zero temperature. At $\nu = 1$, a disordered chiral spin liquid is expected at intermediate values of interaction $U/t \sim 10$ whereas a 120° spiral antiferromagnetic order appears for strong interactions $U/t \gtrsim 12$ [28–46]. Moreover, the ground-state properties have recently been analyzed when the system is doped away from $\nu = 1$ [47]. However, we do not focus on the magnetic ground-state properties but on the finite temperatures ones, see also Refs. [37,48]. In the context of cold atoms in optical lattices, magnetic correlations induced by propagation of fermions at high temperatures has been previously suggested for the square lattice [49].

Our Letter highlights the importance of magnetic polarons in correlated Mott insulators [50–61]. Most of the previous studies of magnetic polarons in the Fermi-Hubbard model focused on the square lattice. They are believed to play a crucial role in unusual properties of high- T_c cuprates, including both the pseudogap regime and the d -wave superconductivity. Magnetic polarons on triangular lattices have also been a subject of theoretical studies [62–65]. It is expected that they also play an important role in defining properties of moiré materials. Their relevance for moiré materials has been suggested previously in Refs. [64,66–68].

Emergence of magnetic interactions from kinetic frustration in triangular lattices. To show the appearance of magnetic interactions from kinetic frustration at finite temperature, we will consider spin- $\frac{1}{2}$ fermions described by a single-band Fermi-Hubbard model,

$$H = -t \sum_{\langle i,j \rangle, \sigma} (c_{i,\sigma}^\dagger c_{j,\sigma} + \text{H.c.}) + U \sum_i n_{i,\uparrow} n_{i,\downarrow} - \frac{h}{2} \sum_i (n_{i,\uparrow} - n_{i,\downarrow}), \quad (1)$$

where U is the on-site repulsion, t is the hopping strength, and h is an external magnetic field. We define the filling of the system $\nu = 1 + \epsilon$, and we study the magnetic phases at finite temperature whereas changing the doping of the system from a hole-doped regime ($\epsilon < 0$) to a doublon-doped one ($\epsilon > 0$).

In the strongly interacting regime $U/t \rightarrow \infty$ for $\nu = 1$, the magnetic properties of the system are accurately described by a model of decoupled spins that can be polarized by a magnetic field on the order of temperature. However, if the system is doped away from $\nu = 1$, the movement of charge carriers can induce different forms of magnetism. In a nonbipartite geometry, the propagation of a single fermionic hole is frustrated in a polarized background [21,63,64,69]. This can be seen from a high- T expansion in the strongly interacting regime. Let us consider a spin-polarized background with a single hole propagating through it. By fixing the initial and final points of the propagation, we have two sets of paths characterized by order n of the high- T expansion in βt . Since the fermionic hole has an effective negative hopping [21,63,64,69], we see that odd paths contribute with an opposite sign than even paths. This gives a destructive interference pattern in the hole propagation. This concept is known as kinetic frustration since the hole cannot get the full kinetic energy associated with the geometry [21,69]. However, if the background is not fully spin polarized, then the destructive interference is suppressed

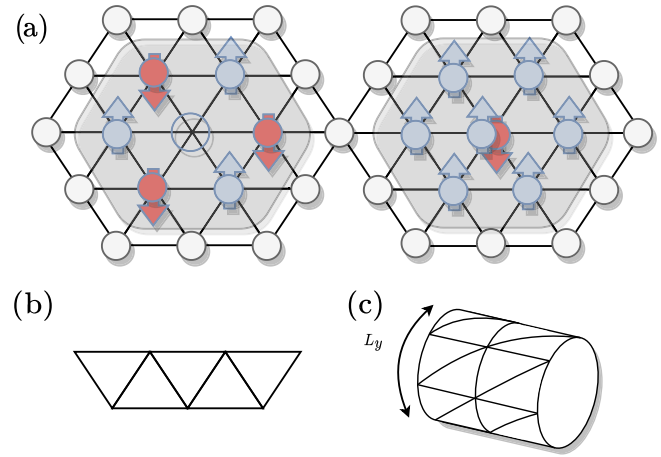


FIG. 1. Triangular lattice geometries analyzed in this paper: (a) 2d lattice (Monte Carlo), (b) zigzag ladder, and (c) four- and six-legged triangular cylinders (tensor network calculations). For the filling factor $\nu = 1$ and at temperatures much larger than the superexchange interaction $k_B T > J$, we find a system of essentially decoupled spins. However, when a single hole (doublon) is introduced on top of the spin incoherent Mott insulator, antiferromagnetic (ferromagnetic) correlations appear surrounding it, see panel (a).

when different hole trajectories result in distinguishable spin configurations. Thus, kinetic energy of a hole can be lowered by inducing antiferromagnetic spin correlations around it. This effect is commonly referred to as antiferromagnetic correlations releasing kinetic frustration for a single hole. It underlies the effective antiferromagnetic interactions in hole-doped Mott insulators in triangular lattices. This effect is closely related to formation of a hole-magnon-bound state in the case of spin-polarized Mott insulators in triangular lattices discussed previously in Refs. [63,64]. When we consider the electron-doped regime ($\nu > 1$), the propagation of doublons in the case of spin-polarized background is not frustrated since they effectively have a positive hopping. Furthermore, different doublon trajectories interfere constructively, in the case of ferromagnetic background but not in the antiferromagnetic environment. In the latter case, different trajectories lead to distinguishable spin configurations. This induces an effective ferromagnetic interaction at ($\nu > 1$) [49,70]. Note that this transition between antiferromagnetic and ferromagnetic interactions by changing the doping at $\nu = 1$ can only occur in a nonbipartite geometry. In a bipartite, one there cannot be a destructive interference pattern since all paths contribute with the same sign in the high- T expansion. The appearance of kinetic magnetism has strong consequences in the magnetic properties of the system at finite temperature. When the typical temperatures are much higher than the superexchange interaction $J = 4t^2/U$, we expect a paramagnetic phase at $\nu = 1$. However, if the temperature is on the order of the hopping strength $k_B T \sim t$, we still expect to see the tendency to Haerter-Shastry antiferromagnetism in the hole-doped regime ($\nu < 1$) and Nagaoka ferromagnetism in the electron-doped one ($\nu > 1$). In order to unravel the effects of kinetic magnetism at zero and finite temperature, we will employ unbiased tensor network and high-temperature expansion quantum Monte Carlo simulations, see Fig. 1. In

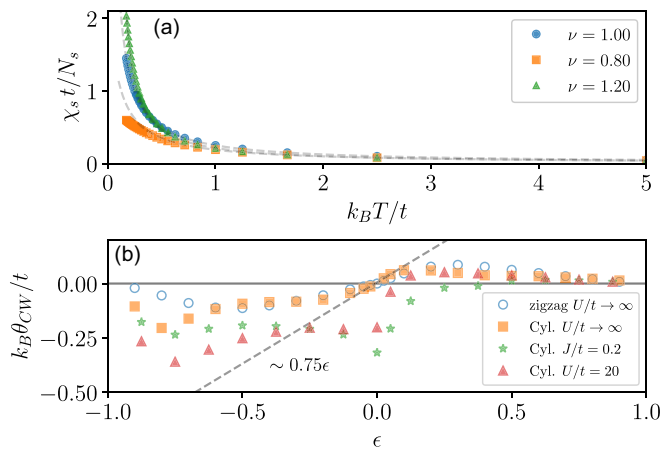


FIG. 2. Panel (a): Magnetic susceptibility per site as a function of temperature for three different dopings $\nu = 1 + \epsilon$ corresponding to a system with exactly one electron per site ($\epsilon = 0$), a hole-doped system ($\epsilon < 0$), and a doublon-doped one ($\epsilon > 0$) in a zigzag ladder 20×2 . The dashed lines correspond to fits using the Curie-Weiss law. Panel (b): Curie-Weiss temperature θ_{CW} as a function of doping $\nu = 1 + \epsilon$ at $h = 0$ for a 20×2 zigzag ladder (empty circles) and a 10×4 triangular cylinder (filled symbols) at different values of the on-site interaction U/t . Simulations with the tJ model (circles, squares, and stars) are performed by projecting out doublons (holes) for $\nu > 1$ ($\nu < 1$). On the other hand, triangles correspond to simulations of the full Fermi-Hubbard model. The dashed line indicates the linear dependence of the Curie-Weiss temperature with doping close to one electron per site for $U/t \rightarrow \infty$.

tensor networks simulations, we use purification to represent the finite temperature density matrix as a matrix product state in a doubled Hilbert space with bond dimension $\chi = 512$. We start by constructing an infinite temperature state in the canonical ensemble fixing the total number of particles but not the magnetization [71], and then we progressively cool down the system by applying an infinitesimal ($\delta\beta = 0.05$) Boltzmann factor using the W_t ($W_{t|}$) technique in Fig. 2 (Fig. 4) [72]. In a path-integral picture, our Monte Carlo method samples the imaginary time paths of a hole or a doublon in a $\nu = 1$ system with spin imbalance. The spin degrees of freedom are integrated out analytically, and only the paths are sampled. This leads to a low sampling noise for the spin correlations [49], which allows us to achieve temperatures down to $k_B T \sim 0.2t$ and system sizes up to several thousand sites. For details, see the Supplemental Material [73].

Magnetic susceptibility at finite temperature. The tendency towards magnetic order can be inferred from the magnetic susceptibility χ_s of the system. Upon doping, we see an enhancement (suppression) of magnetic susceptibility above (below) $\nu = 1$ at low temperatures, see Fig. 2 panel (a). This indicates the appearance of antiferromagnetic (ferromagnetic) correlations in the hole (electron) doped regime as expected. On the other hand, we observe a suppression of magnetic susceptibility above and below $\nu = 1$ at high temperatures. This can be understood as holes and doublons are spinless particles that effectively reduce the possible total spin of the system, thus, reducing the magnetic susceptibility.

In order to quantify the different contributions to the magnetic susceptibility, we fit the Curie-Weiss law $\chi_s t / N_s =$

$\frac{C}{T - \theta_{\text{CW}}}$ to our data at intermediate temperatures ($5 \gtrsim k_B T / t \gtrsim 1$), where C is the Curie constant and θ_{CW} is the Curie-Weiss temperature. The Curie-Weiss temperature denotes the tendency towards ferromagnetism ($\theta_{\text{CW}} > 0$) or antiferromagnetism ($\theta_{\text{CW}} < 0$). However at high temperatures, the constant C dominates the dependence of the magnetic susceptibility with temperature. The Curie constant can be easily determined by taking into account the contribution of each spin to the spin susceptibility, $C = S(S+1)(1 - |\epsilon|)/3$. Thus, it decreases upon doping since the number of spins is reduced. On the other hand, the Curie-Weiss temperature changes sign at $\nu = 1$ confirming the transition from antiferromagnetic to ferromagnetic interactions in the system, see Fig. 2 panel (b). We observe a linear tendency of the Curie-Weiss temperature with ϵ close to $\nu = 1$, $\theta_{\text{CW}}/t \sim 0.75\epsilon$, which confirms the appearance of kinetic magnetism.

To establish closer connections with experiments, we study the effects of a finite but large on-site interaction on the Curie-Weiss temperature. We choose the value $U/t = 20$ since it is relevant for both TMDC heterostructures and cold atom systems. The finite on-site interaction enhances the antiferromagnetic interactions, increasing the absolute value of the Curie-Weiss temperature on the hole-doped side, see Fig. 2(b). Moreover, ferromagnetic correlations are suppressed, and we observe that the transition from antiferro- to ferromagnetic correlations is shifted to finite electron doping $\nu_c > 1$. This is in accordance with the experimental observation in Refs. [22,23]. We also perform a comparison between the Curie-Weiss temperature extracted from the tJ model and the full Fermi-Hubbard model. The full Fermi-Hubbard model compared to the tJ shows stronger antiferromagnetic (ferromagnetic) correlations in the hole- (electron-) doped side and weaker antiferromagnetic correlations at $\nu = 1$, see Fig. 2(b).

Nonlinear response to magnetic field. To elucidate the kinetically induced many-body phases appearing in the $U/t \rightarrow \infty$ limit, we study the nonlinear response to an external magnetic field at zero temperature, see the Supplemental Material [73] for a finite temperature study. We define the degree of polarization (DOP) of the system as two times the magnetization per single fermion in the system $\text{DOP} = 2m/(1 - |\epsilon|)$. As shown in Fig. 3, the system resists fully polarizing upon hole doping even at zero temperature. We observe a large saturation magnetic field of the order of the hopping strength. At low dopings ($1 > \nu \gtrsim 0.9$), the system has a sudden drop of polarization at a critical magnetic field determined by the binding energy of the hole-magnon bound state $h_c/t \sim 0.5t$. This effect resembles the one expected in metamagnetic materials. At this point, the system has a first-order phase transition from a fully polarized phase to a magnetic polaron gas. In this phase, each hole is attached with a spin flip (magnon) forming a hole-magnon bound state. Due to this effect the polarization in the magnetic polaron gas is linked to the hole density by $P_0 = (1 - 3|\epsilon|)/(1 - |\epsilon|)$. Therefore, this phase is characterized by a fixed polarization and a gap to single-particle excitations. As the hole density increases, the polarization plateau and the jump of polarization start to disappear due to the overlap of the magnetic polarons, see curves with $\nu < 0.89$. At these densities, we cannot rely on the simple picture of a weakly interacting gas of magnetic polarons. Instead of a sharp transition from a fully polarized state to a magnetic

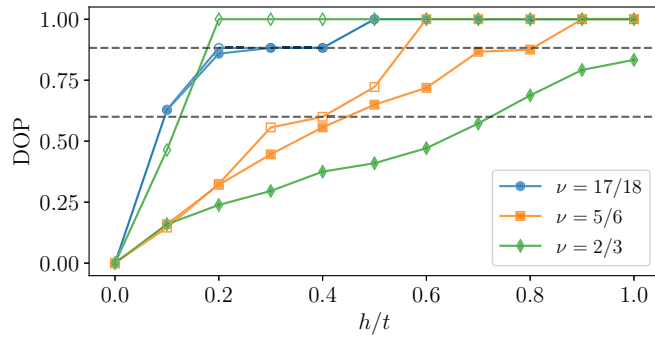


FIG. 3. Degree of polarization (DOP) of an infinite triangular cylinder of $L_y = 6$ as a function of the external magnetic-field h at different filling factors ν at $J/t = 0$ and at zero temperature. Filled (empty) symbols correspond to the case $V/t = 0$ ($V/t = 6$). The dashed line indicates the polarization plateau expected for the magnetic polaron gas at $\nu = 17/18, 5/6$.

polaron gas, we observe a smooth crossover in a wide range of magnetic field. In this region of magnetic field, we expect a phase coexistence between magnetic polarons and bare holes. This phase coexistence is accompanied by a sudden change in slope in the degree of polarization as a function of magnetic field.

At small magnetic fields, the system linearly polarizes with the magnetic field, see Fig. 3. In this regime, we observe phase separation into two domains with different hole densities. One domain has zero doping and is fully spin polarized, the other domain is “hole rich” and exhibits antiferromagnetic correlations. Appearance of phase separation indicates effective attractive interaction between magnetic polarons. Although in the “plain-vanilla” Fermi-Hubbard model we find global phase separation, we expect that introducing additional interactions, such as long-range interactions, can result in other interesting phases, including the paired state and stripe order. The former may be relevant to superconductivity in moiré systems. We point out the unusual feature of the effective interaction between magnetic polarons: it depends on the magnetic field. By increasing magnetic field, there is a competition between the effective antiferromagnetic interactions and the Zeeman energy gain. This reduces the size of the spin bag down to a single spin flip at a critical magnetic field. At this point we have a transition to a magnetic polaron gas. We observe that this critical magnetic field coincides with the field at which multiple holes are confined inside a single bag. Thus, indicating a transition from effective attractive to repulsive interactions between magnetic polarons.

Finally, we study the effects of including a density-density nearest-neighbor repulsive interaction with strength V in Hamiltonian (1). In Fig. 3, we show how the nonlinear magnetic response changes when such interaction is included. Kinetic antiferromagnetism is robust with respect to this interaction at small hole dopings and the polarization curve is not altered. However, at rational fillings, such as $\nu = 2/3$, we observe a fast polarization of the system with magnetic field when a nonlocal interaction is included. This effect can be explained by the formation of a Mott-Wigner state in which the holes become immobile, leading to a strong suppression of kinetic magnetism.

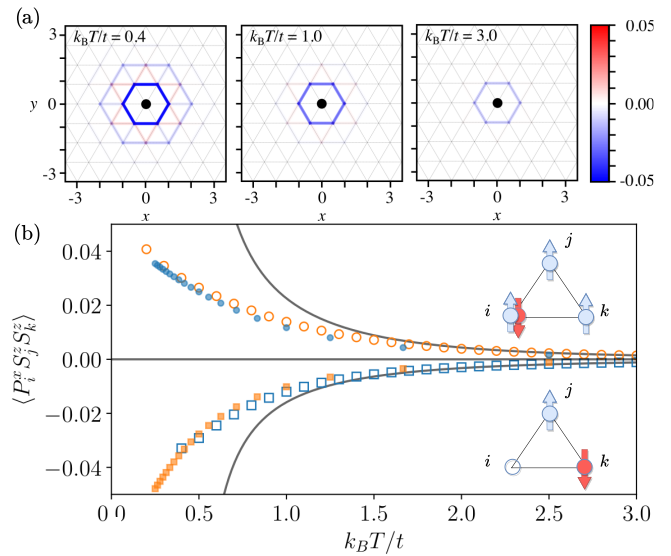


FIG. 4. Panel (a): Charge-spin-spin correlation function in a full two-dimensional triangular 20×20 lattice obtained via Monte Carlo simulations at three different temperatures. The black circle denotes the hole position, and the links show the strength of the spin-spin correlations with color. Panel (b): Charge-spin-spin correlator as a function of temperature for a six-legged triangular cylinder with $L_x = 6$ with a single hole (blue dots) and with a single doublon (orange squares). P_i^x denotes a projector, which fixes the charge position at site i . The filled (open) symbols correspond to the tensor network (Monte Carlo) results. Continuous lines show the high- T expansion. We also show a schematic of the antiferro- and ferromagnetic correlations surrounding the hole and the doublon, respectively.

Implications for cold atoms experiments. Our results are not only relevant for TMDC heterostructures, but they also have strong implications for ultracold atomic systems in triangular optical lattices [22,74,75]. Specifically, spin-charge correlations could be accessed in systems with a quantum gas microscope [75–85]. These experimental systems can be used to measure higher-order correlation functions. In Fig. 4, we present the plaquette charge-spin-spin correlation function in the hole-doped regime ($\nu < 1$) and the electron-doped one ($\nu > 1$) as a function of temperature. In the hole- (electron-) doped regime antiferromagnetic (ferromagnetic) correlations appear in the system as it is cooled down. Similar correlations have been observed in the hole-doped regime [86]. In the Supplemental Material [73], we also provide an analytical high-temperature expansion for the charge-spin-spin correlation function, which compares well with the numerical calculations for temperatures $k_B T \gtrsim t$, see Fig. 4. Thus, we conclude that site-resolved correlations could be used as a fingerprint of kinetic magnetism.

Outlook. Our Letter shows how effective magnetic interactions arise due to the motion of charge carriers in a frustrated geometry at finite and zero temperatures. In the strongly interacting regime $U/t \rightarrow \infty$, the superexchange interaction is suppressed. However, effective magnetic interactions due to the motion of charge carriers are relevant when the system is doped away from $\nu = 1$. Due to kinetic frustration, these effective magnetic interactions change sign close to $\nu = 1$.

Thus, a magnetic transition from an antiferromagnet to a ferromagnet is expected when moving from a hole-doped to an electron-doped regime. We also point out the relationship of these effective magnetic interactions with the formation of magnetic polarons. We observe the formation of a magnetic polaron gas at temperatures below the hopping strength.

When this Letter was being finalized, we learned about papers [67,68] that addressed related questions.

Acknowledgments. We acknowledge useful discussions with W. Bakr, A. Bohrdt, M. Greiner, F. Grusdt, E.-A. Kim, K. Sengstock, G. Refael, and I. Esterlis. We thank M. Greiner's group for sharing their experimental results with us prior to publication. I.M. acknowledges support from Grant No. PID2020-114626GB-I00 from the MICIN/AEI/10.13039/501100011033 and Secretaria d'Universitats i Recerca del Departament d'Empresa i

Coneixement de la Generalitat de Catalunya, cofunded by the European Union Regional Development Fund within the ERDF Operational Program of Catalunya (Project No. QuantumCat, Ref. 001-P-001644). I.M. acknowledges the Theoretical Physics Institute at ETH for hospitality, where part of this work was completed. M.K.-N. acknowledges support by the EU Horizon 2020 program through the ERC Advanced Grant QUENOCOBA No. 742102 and from the DFG (German Research Foundation) under Germany's Excellence Strategy-EXC-2111-390814868. E.D. acknowledges support by the SNSF Project No. 200021_212899 and the ARO Grant No. W911NF-20-1-0163. The work of L.C., T.S. and A.I. was supported by the Swiss National Science Foundation (SNSF) under Grant No. 200021-204076. Tensor Network computations have been performed using TeNPy [87].

-
- [1] D. D. Awschalom and M. E. Flatté, Challenges for semiconductor spintronics, *Nat. Phys.* **3**, 153 (2007).
- [2] S. A. Wolf, D. D. Awschalom, R. A. Buhrman, J. M. Daughton, S. von Molnár, M. L. Roukes, A. Y. Chtchelkanova, and D. M. Treger, Spintronics: A spin-based electronics vision for the future, *Science* **294**, 1488 (2001).
- [3] H. Ohno, D. Chiba, F. Matsukura, T. Omiya, E. Abe, T. Dietl, Y. Ohno, and K. Ohtani, Electric-field control of ferromagnetism, *Nature (London)* **408**, 944 (2000).
- [4] A. Chattopadhyay, S. Das Sarma, and A. J. Millis, Transition Temperature of Ferromagnetic Semiconductors: A Dynamical Mean Field Study, *Phys. Rev. Lett.* **87**, 227202 (2001).
- [5] A. Kaminski and S. Das Sarma, Polaron Percolation in Diluted Magnetic Semiconductors, *Phys. Rev. Lett.* **88**, 247202 (2002).
- [6] H. Boukari, P. Kossacki, M. Bertolini, D. Ferrand, J. Cibert, S. Tatarenko, A. Wasiela, J. A. Gaj, and T. Dietl, Light and Electric Field Control of Ferromagnetism in Magnetic Quantum Structures, *Phys. Rev. Lett.* **88**, 207204 (2002).
- [7] T. Jungwirth, J. Sinova, J. Mašek, J. Kučera, and A. H. MacDonald, Theory of ferromagnetic (iii,mn)v semiconductors, *Rev. Mod. Phys.* **78**, 809 (2006).
- [8] H.-J. Lee, E. Helgren, and F. Hellman, Gate-controlled magnetic properties of the magnetic semiconductor (zn,co)o, *Appl. Phys. Lett.* **94**, 212106 (2009).
- [9] Y. Nishitani, D. Chiba, M. Endo, M. Sawicki, F. Matsukura, T. Dietl, and H. Ohno, Curie temperature versus hole concentration in field-effect structures of Ga_{1-x}Mn_xAs, *Phys. Rev. B* **81**, 045208 (2010).
- [10] M. Sawicki, D. Chiba, A. Korbecka, Y. Nishitani, J. A. Majewski, F. Matsukura, T. Dietl, and H. Ohno, Experimental probing of the interplay between ferromagnetism and localization in (ga, mn)as, *Nat. Phys.* **6**, 22 (2010).
- [11] L. Li, Y. Guo, X. Y. Cui, R. Zheng, K. Ohtani, C. Kong, A. V. Ceguerra, M. P. Moody, J. D. Ye, H. H. Tan, C. Jagadish, H. Liu, C. Stampfl, H. Ohno, S. P. Ringer, and F. Matsukura, Magnetism of co-doped zno epitaxially grown on a zno substrate, *Phys. Rev. B* **85**, 174430 (2012).
- [12] H. Wen Chang, S. Akita, F. Matsukura, and H. Ohno, Hole concentration dependence of the curie temperature of (Ga, Mn)Sb in a field-effect structure, *Appl. Phys. Lett.* **103**, 142402 (2013).
- [13] F. Matsukura, Y. Tokura, and H. Ohno, Control of magnetism by electric fields, *Nat. Nanotechnol.* **10**, 209 (2015).
- [14] C. H. Ahn, A. Bhattacharya, M. Di Ventura, J. N. Eckstein, C. D. Frisbie, M. E. Gershenson, A. M. Goldman, I. H. Inoue, J. Mannhart, A. J. Millis, A. F. Morpurgo, D. Natelson, and J.-M. Triscone, Electrostatic modification of novel materials, *Rev. Mod. Phys.* **78**, 1185 (2006).
- [15] A. J. Millis, B. I. Shraiman, and R. Mueller, Dynamic Jahn-Teller Effect and Colossal Magnetoresistance in La_{1-x}Sr_xMnO₃, *Phys. Rev. Lett.* **77**, 175 (1996).
- [16] Y. Tokura (Ed.), *Colossal Magnetoresistive Oxides*, Advances in Condensed Matter Science (Taylor and Francis, London, 2000).
- [17] M. B. Salamon and M. Jaime, The physics of manganites: Structure and transport, *Rev. Mod. Phys.* **73**, 583 (2001).
- [18] Y. Tokura, Critical features of colossal magnetoresistive manganites, *Rep. Prog. Phys.* **69**, 797 (2006).
- [19] Y. Nagaoka, Ferromagnetism in a narrow, almost half-filled s band, *Phys. Rev.* **147**, 392 (1966).
- [20] D. J. Thouless, Exchange in solid ³He and the Heisenberg Hamiltonian, *Pro. Phys. Soc., London* **86**, 893 (1965).
- [21] J. O. Haerter and B. S. Shastry, Kinetic Antiferromagnetism in the Triangular Lattice, *Phys. Rev. Lett.* **95**, 087202 (2005).
- [22] M. Xu, L. H. Kendrick, A. Kale, Y. Gang, G. Ji, R. T. Scalettar, M. Lebrat, and M. Greiner, Doping a frustrated fermi-hubbard magnet, [arXiv:2212.13983](https://arxiv.org/abs/2212.13983).
- [23] Y. Tang, L. Li, T. Li, Y. Xu, S. Liu, K. Barmak, K. Watanabe, T. Taniguchi, A. H. MacDonald, J. Shan, and K. F. Mak, Simulation of hubbard model physics in WSe₂/WS₂ moiré superlattices, *Nature (London)* **579**, 353 (2020).
- [24] L. Ciorciaro, T. Smolenski, I. Morera, N. Kiper, S. Hiestand, M. Kroner, Y. Zhang, K. Watanabe, T. Taniguchi, E. Demler, and A. Imamoglu, Kinetic magnetism in triangular moiré materials, (2023), [arXiv:2305.02150](https://arxiv.org/abs/2305.02150) [cond-mat.str-el].
- [25] Y. Zhang, N. F. Q. Yuan, and L. Fu, Moiré quantum chemistry: Charge transfer in transition metal dichalcogenide superlattices, *Phys. Rev. B* **102**, 201115(R) (2020).
- [26] M. S. Hossain, M. K. Ma, K. A. Villegas Rosales, Y. J. Chung, L. N. Pfeiffer, K. W. West, K. W. Baldwin, and M. Shayegan, Observation of spontaneous ferromagnetism in a

- two-dimensional electron system, *Proc. Natl. Acad. Sci. USA* **117**, 32244 (2020).
- [27] K.-S. Kim, C. Murthy, A. Pandey, and S. A. Kivelson, Interstitial-Induced Ferromagnetism in a Two-Dimensional Wigner Crystal, *Phys. Rev. Lett.* **129**, 227202 (2022).
- [28] T. Koretsune, Y. Motome, and A. Furusaki, Exact diagonalization study of mott transition in the hubbard model on an anisotropic triangular lattice, *J. Phys. Soc. Jpn.* **76**, 074719 (2007).
- [29] P. Sahebsara and D. Sénéchal, Hubbard Model on the Triangular Lattice: Spiral Order and Spin Liquid, *Phys. Rev. Lett.* **100**, 136402 (2008).
- [30] R. T. Clay, H. Li, and S. Mazumdar, Absence of Superconductivity in the Half-Filled Band Hubbard Model on the Anisotropic Triangular Lattice, *Phys. Rev. Lett.* **101**, 166403 (2008).
- [31] T. Watanabe, H. Yokoyama, Y. Tanaka, and J. Inoue, Predominant magnetic states in the hubbard model on anisotropic triangular lattices, *Phys. Rev. B* **77**, 214505 (2008).
- [32] D. Galanakis, T. D. Stanescu, and P. Phillips, Mott transition on a triangular lattice, *Phys. Rev. B* **79**, 115116 (2009).
- [33] T. Yoshioka, A. Koga, and N. Kawakami, Quantum Phase Transitions in the Hubbard Model on a Triangular Lattice, *Phys. Rev. Lett.* **103**, 036401 (2009).
- [34] H.-Y. Yang, A. M. Läuchli, F. Mila, and K. P. Schmidt, Effective Spin Model for the Spin-Liquid Phase of the Hubbard Model on the Triangular Lattice, *Phys. Rev. Lett.* **105**, 267204 (2010).
- [35] J. Kokalj and R. H. McKenzie, Thermodynamics of a Bad Metal–Mott Insulator Transition in the Presence of Frustration, *Phys. Rev. Lett.* **110**, 206402 (2013).
- [36] A. Yamada, Magnetic properties and mott transition in the hubbard model on the anisotropic triangular lattice, *Phys. Rev. B* **89**, 195108 (2014).
- [37] G. Li, A. E. Antipov, A. N. Rubtsov, S. Kirchner, and W. Hanke, Competing phases of the hubbard model on a triangular lattice: Insights from the entropy, *Phys. Rev. B* **89**, 161118 (2014).
- [38] L. F. Tocchio, C. Gros, R. Valentí, and F. Becca, One-dimensional spin liquid, collinear, and spiral phases from uncoupled chains to the triangular lattice, *Phys. Rev. B* **89**, 235107 (2014).
- [39] M. Laubach, R. Thomale, C. Platt, W. Hanke, and G. Li, Phase diagram of the hubbard model on the anisotropic triangular lattice, *Phys. Rev. B* **91**, 245125 (2015).
- [40] R. V. Mishmash, I. González, R. G. Melko, O. I. Motrunich, and M. P. A. Fisher, Continuous mott transition between a metal and a quantum spin liquid, *Phys. Rev. B* **91**, 235140 (2015).
- [41] T. Shirakawa, T. Tohyama, J. Kokalj, S. Sota, and S. Yunoki, Ground-state phase diagram of the triangular lattice hubbard model by the density-matrix renormalization group method, *Phys. Rev. B* **96**, 205130 (2017).
- [42] A. Szasz, J. Motruk, M. P. Zaletel, and J. E. Moore, Chiral Spin Liquid Phase of the Triangular Lattice Hubbard Model: A Density Matrix Renormalization Group Study, *Phys. Rev. X* **10**, 021042 (2020).
- [43] A. Szasz and J. Motruk, Phase diagram of the anisotropic triangular lattice hubbard model, *Phys. Rev. B* **103**, 235132 (2021).
- [44] T. Cookmeyer, J. Motruk, and J. E. Moore, Four-Spin Terms and the Origin of the Chiral Spin Liquid in Mott Insulators on the Triangular Lattice, *Phys. Rev. Lett.* **127**, 087201 (2021).
- [45] A. Wietek, R. Rossi, F. Šimkovic, IV, M. Klett, P. Hansmann, M. Ferrero, E. M. Stoudenmire, T. Schäfer, and A. Georges, Mott Insulating States with Competing Orders in the Triangular Lattice Hubbard Model, *Phys. Rev. X* **11**, 041013 (2021).
- [46] Bin-Bin Chen, Z. Chen, Shou-Shu Gong, D. N. Sheng, W. Li, and A. Weichselbaum, Quantum spin liquid with emergent chiral order in the triangular-lattice hubbard model, *Phys. Rev. B* **106**, 094420 (2022).
- [47] Z. Zhu, D. N. Sheng, and A. Vishwanath, Doped mott insulators in the triangular-lattice hubbard model, *Phys. Rev. B* **105**, 205110 (2022).
- [48] J. O. Haerter, M. R. Peterson, and B. S. Shastry, Finite-temperature properties of the triangular lattice $t-j$ model and applications to Na_xCoO_2 , *Phys. Rev. B* **74**, 245118 (2006).
- [49] M. Kánász-Nagy, I. Lovas, F. Grusdt, D. Greif, M. Greiner, and E. A. Demler, Quantum correlations at infinite temperature: The dynamical nagaoka effect, *Phys. Rev. B* **96**, 014303 (2017).
- [50] E. L. Nagaev L. N. Bulaevskii and D. I. Khomskii, A new type of auto-localized state of a conduction electron in an antiferromagnetic semiconductor, *Zh. Eksp. Teor. Fiz.* **54**, 1562 (1968).
- [51] S. A. Trugman, Interaction of holes in a hubbard antiferromagnet and high-temperature superconductivity, *Phys. Rev. B* **37**, 1597 (1988).
- [52] S. Schmitt-Rink, C. M. Varma, and A. E. Ruckenstein, Spectral Function of Holes in a Quantum Antiferromagnet, *Phys. Rev. Lett.* **60**, 2793 (1988).
- [53] B. I. Shraiman and E. D. Siggia, Mobile Vacancies in a Quantum Heisenberg Antiferromagnet, *Phys. Rev. Lett.* **61**, 467 (1988).
- [54] S. Sachdev, Hole motion in a quantum néel state, *Phys. Rev. B* **39**, 12232 (1989).
- [55] C. L. Kane, P. A. Lee, and N. Read, Motion of a single hole in a quantum antiferromagnet, *Phys. Rev. B* **39**, 6880 (1989).
- [56] E. Dagotto, A. Moreo, and T. Barnes, Hubbard model with one hole: Ground-state properties, *Phys. Rev. B* **40**, 6721 (1989).
- [57] A. Auerbach, *Interacting Electrons and Quantum Magnetism*, 1st ed., Graduate Texts in Contemporary Physics (Springer, New York, 1998).
- [58] E. L. Nagaev, Magnetic polarons (ferrons) of complicated structure, *JETP Lett.* **74**, 431 (2001).
- [59] F. Grusdt, M. Kánász-Nagy, A. Bohrdt, C. S. Chiu, G. Ji, M. Greiner, D. Greif, and E. Demler, Parton Theory of Magnetic Polarons: Mesonic Resonances and Signatures in Dynamics, *Phys. Rev. X* **8**, 011046 (2018).
- [60] J. Koepsell, J. Vijayan, P. Sompet, F. Grusdt, T. A. Hilker, E. Demler, G. Salomon, I. Bloch, and C. Gross, Imaging magnetic polarons in the doped fermi–hubbard model, *Nature (London)* **572**, 358 (2019).
- [61] D. Soriano and M. I. Katsnelson, Magnetic polaron and antiferromagnetic-ferromagnetic transition in doped bilayer CrI_3 , *Phys. Rev. B* **101**, 041402(R) (2020).
- [62] S. V. Iordanskil and A. V. Smirnov, Magnetic structures in the Hubbard model with nearly half-filled band for nonalternating lattices, *Zh. Eksp. Teor. Fiz.* **79**, 1942 (1980).
- [63] S.-S. Zhang, W. Zhu, and C. D. Batista, Pairing from strong repulsion in triangular lattice hubbard model, *Phys. Rev. B* **97**, 140507(R) (2018).
- [64] I. Morera, A. Bohrdt, W. W. Ho, and E. Demler, Attraction from frustration in ladder systems, [arxiv:2106.09600](https://arxiv.org/abs/2106.09600).

- [65] J. van de Kraats, K. K. Nielsen, and G. M. Bruun, Holes and magnetic polarons in a triangular lattice antiferromagnet, *Phys. Rev. B* **106**, 235143 (2022).
- [66] M. Davydova, Y. Zhang, and L. Fu, Itinerant spin polaron and metallic ferromagnetism in semiconductor moiré superlattices, [arxiv:2206.01221](https://arxiv.org/abs/2206.01221).
- [67] K. Lee, P. Sharma, O. Vafek, and H. J. Changlani, Triangular lattice hubbard model physics at intermediate temperatures, [arxiv:2209.00664](https://arxiv.org/abs/2209.00664).
- [68] Y. Zhang and L. Fu, Pseudogap metal and magnetization plateau from doping moiré mott insulator, [arXiv:2209.05430](https://arxiv.org/abs/2209.05430).
- [69] C. N. Sposetti, B. Bravo, A. E. Trumper, C. J. Gazza, and L. O. Manuel, Classical Antiferromagnetism in Kinetically Frustrated Electronic Models, *Phys. Rev. Lett.* **112**, 187204 (2014).
- [70] T. Hanisch, B. Kleine, A. Ritzl, and E. Müller-Hartmann, Ferromagnetism in the hubbard model: Instability of the nagaoka state on the triangular, honeycomb and kagome lattices, *Ann. Phys. (NY)* **507**, 303 (1995).
- [71] T. Barthel, Matrix product purifications for canonical ensembles and quantum number distributions, *Phys. Rev. B* **94**, 115157 (2016).
- [72] M. P. Zaletel, R. S. K. Mong, C. Karrasch, J. E. Moore, and F. Pollmann, Time-evolving a matrix product state with long-ranged interactions, *Phys. Rev. B* **91**, 165112 (2015).
- [73] See Supplemental Material at <https://link.aps.org/supplemental/10.1103/PhysRevResearch.5.L022048> for details on the tensor network and Monte Carlo simulations; an analytical expression for the high-temperature expansion of the charge-spin-spin correlator; a discussion on the effective magnetic interactions induced by kinetic frustration; the nonlinear magnetic response at finite temperature; the degree of polarization dependence with the filling factor; and an analysis of the system at low magnetic fields, which includes Ref. [88].
- [74] J. Struck, C. Ölschläger, R. L. Targat, P. Soltan-Panahi, A. Eckardt, M. Lewenstein, P. Windpassinger, and K. Sengstock, Quantum simulation of frustrated classical magnetism in triangular optical lattices, *Science* **333**, 996 (2011).
- [75] J. Yang, L. Liu, J. Mongkolkiattichai, and P. Schauss, Site-resolved imaging of ultracold fermions in a triangular-lattice quantum gas microscope, *PRX Quantum* **2**, 020344 (2021).
- [76] W. S. Bakr, J. I. Gillen, A. Peng, S. Fölling, and M. Greiner, A quantum gas microscope for detecting single atoms in a hubbard-regime optical lattice, *Nature (London)* **462**, 74 (2009).
- [77] J. F. Sherson, C. Weitenberg, M. Endres, M. Cheneau, I. Bloch, and S. Kuhr, Single-atom-resolved fluorescence imaging of an atomic mott insulator, *Nature (London)* **467**, 68 (2010).
- [78] M. F. Parsons, F. Huber, A. Mazurenko, C. S. Chiu, W. Setiawan, K. Wooley-Brown, S. Blatt, and M. Greiner, Site-Resolved Imaging of Fermionic ${}^6\text{Li}$ in an Optical Lattice, *Phys. Rev. Lett.* **114**, 213002 (2015).
- [79] L. W. Cheuk, M. A. Nichols, M. Okan, T. Gersdorf, V. V. Ramasesh, W. S. Bakr, T. Lompe, and M. W. Zwierlein, Quantum-Gas Microscope for Fermionic Atoms, *Phys. Rev. Lett.* **114**, 193001 (2015).
- [80] A. Omran, M. Boll, T. A. Hilker, K. Kleinlein, G. Salomon, I. Bloch, and C. Gross, Microscopic Observation of Pauli Blocking in Degenerate Fermionic Lattice Gases, *Phys. Rev. Lett.* **115**, 263001 (2015).
- [81] E. Haller, J. Hudson, A. Kelly, D. A. Cotta, B. Peaudecerf, G. D. Bruce, and S. Kuhr, Single-atom imaging of fermions in a quantum-gas microscope, *Nat. Phys.* **11**, 738 (2015).
- [82] G. J. A. Edge, R. Anderson, D. Jervis, D. C. McKay, R. Day, S. Trotzky, and J. H. Thywissen, Imaging and addressing of individual fermionic atoms in an optical lattice, *Phys. Rev. A* **92**, 063406 (2015).
- [83] D. Greif, M. F. Parsons, A. Mazurenko, C. S. Chiu, S. Blatt, F. Huber, G. Ji, and M. Greiner, Site-resolved imaging of a fermionic mott insulator, *Science* **351**, 953 (2016).
- [84] P. T. Brown, D. Mitra, E. Guardado-Sanchez, P. Schauß, S. S. Kondov, E. Khatami, T. Paiva, N. Trivedi, D. A. Huse, and W. S. Bakr, Spin-imbalance in a 2d fermi-hubbard system, *Science* **357**, 1385 (2017).
- [85] C. Weitenberg, M. Endres, J. F. Sherson, M. Cheneau, P. Schauß, T. Fukuhara, I. Bloch, and S. Kuhr, Single-spin addressing in an atomic mott insulator, *Nature (London)* **471**, 319 (2011).
- [86] D. Garwood, J. Mongkolkiattichai, L. Liu, J. Yang, and P. Schauss, Site-resolved observables in the doped spin-imbalance triangular hubbard model, *Phys. Rev. A* **106**, 013310 (2022).
- [87] J. Hauschild and F. Pollmann, Efficient numerical simulations with Tensor Networks: Tensor Network Python (TeNPy), *SciPost Phys. Lect. Notes*, **5** (2018).
- [88] J. Carlström, N. Prokof'ev, and B. Svistunov, Quantum Walk in Degenerate Spin Environments, *Phys. Rev. Lett.* **116**, 247202 (2016).